Dimensional crossover in Cr-doped Co$_3$BO$_5$

D. L. Mariano[1], M. A. V. Heringer,[1] D. C. Freitas,[1] E. Baggio-Saitovitch,[2]
M. A. Continentino[2], E. C. Passamani[3], and D. R. Sanchez[1,*]

[1]*Instituto de Física, Universidade Federal Fluminense, Campus da Praia Vermelha, 24210-340 Niterói, Rio de Janeiro, Brazil*
[2]*Centro Brasileiro de Pesquisas Físicas, Rua Doutor Xavier Sigaud, 150-Urca 22290-180 Rio de Janeiro, Rio de Janeiro, Brazil*
[3]*Departamento de Física, Universidade Federal do Espírito Santo, Avenida Fernando Ferrari, 514-Goiabeiras 29075-010 Vitória,*
Espírito Santo, Brazil

The crystal structure and the magnetic properties of the Co$_{2.5}$Cr$_{0.5}$BO$_5$ ludwigite have been investigated by x-ray diffraction, magnetization, and specific heat experiments. Cr ions mainly occupy sites 4 of the ludwigite lattice, substituting approximately half of the Co^{3+}. It changes the interatomic distances and favors a high spin state for the remaining Co^{3+} ions. Doping the homometallic Co$_3$BO$_5$ with magnetic Cr drastically increases the magnetic transition temperature from 42 K, for the undoped compound, to 76 K for Co$_{2.5}$Cr$_{0.5}$BO$_5$. The latter contains three different magnetic ions, Co^{2+}, Co^{3+} and Cr^{3+} in high spin states, as evidenced by magnetization measurements. The specific position of Cr in the structure (sites 4) gives rise, according to calculations of the exchange interactions and the Goodenough-Kanamori rules, to a few frustrated magnetic interactions. This is responsible for the high ferrimagnetic ordering temperature of 76 K, when compared to that of the pure compound. The experimental results imply a magnetic structure for the system that we show is consistent with the known interactions and the Goodenough-Kanamori rules. Low temperature specific heat and magnetization measurements reveal that the two-dimensional nature of the magnetism Co$_3$BO$_5$ when doped with Cr acquires a three-dimensional character with a high temperature ferrimagnetic order.

I. INTRODUCTION

The variety of physical behavior displayed by the oxyborates has been attributed to a combination of strong correlations and low-dimensional effects. In particular, ludwigites with formula unit $M_2 M'$BO$_5$ exhibit different physical properties ranging from structural ordering [1], charge ordering [2,3], coexistence of magnetic order and paramagnetism [4], metamagnetic transitions [5], magnetocaloric effect [5], spin-glass [6,7], among others. In relation to their technological applications, some of them can be used as low frequency oscillators [8] or as anodes in lithium or sodium batteries [9].

Structurally, the ludwigites have four nonequivalent crystallographic sites for the metal ions, which are octahedrally coordinated by oxygen ions. The sites corresponding to the same crystallographic positions are arranged in a row along the c axis sharing two of their four edges. According to their structural and magnetic properties, these compounds are generally seen as composed of two subsystems, each one consisting of three coplanar parallel rows of metallic ions along the c axis, known as three-legged ladder . In the $3 - 1 - 3$ ladder, the outer legs contain ions at sites 3 and the central leg ions at sites 1. The octahedra of the same crystalline sites share two edges, while those corresponding to different sites share a vertex. The distance between two different ions in a rung of the $3 - 1 - 3$ ladder is approximately 3.3 Å. Analogously, the $4 - 2 - 4$ ladder with ions at sites 4 and 2 differs with respect to the previous subsystem in that all octahedra sites

are sharing edges. The distance between two different ions in a rung of this ladder is shorter and approximately 2.7 Å.

Among all the ludwigites that have been studied so far, only two of them are homometallic, namely Fe$_3$BO$_5$ [1–3] and Co$_3$BO$_5$ [10]. In these two homometallic ludwigites, the outer legs of the $4 - 2 - 4$ ladder are occupied by trivalent metallic ions, while the remaining sites are occupied by divalent ions. This makes the $4 - 2 - 4$ ladder more interesting since it contains two ions with different valences and also because the distances between ions in a rung of this ladder are the shortest found in the structure. Thus, the strongest magnetic interactions are expected to take place in the $4 - 2 - 4$ ladder.

In the Fe$_3$BO$_5$ ludwigite, a charge order and dimerization of the lattice (long and short bonds in the rungs alternate along the ladder) occur in the ladder $4 - 2 - 4$ at ∼283 K [1–3]. Each rung can be viewed as three Fe^{3+}ions (triad), in a high spin state $S = 5/2$, sharing an extra electron [2]. The $4 - 2 - 4$ ladder orders antiferromagnetically below 112 K, while the $3 - 1 - 3$ ladder remains paramagnetic. Below 76 K, a magnetic order of the whole system takes place and a complex arrangement of the spins is established [2–4]. On the other hand, the homometallic Co$_3$BO$_5$ ludwigite has a unique magnetic transition at 43 K at which the whole system orders. The latter transition temperature is much lower than that of Fe$_3$BO$_5$ [10,11].

This result is intriguing since both compounds have the same structure and similar electronic configurations. Although the magnitude of the involved magnetic moments are different in both compounds, this does not seem to be sufficient to explain the large difference of the magnetic transition

*dalbersanchez@id.uff.br

temperatures. Neutron studies of the Co_3BO_5 ludwigite have shown that, contrary to expectations, Co^{3+} ions at sites 4 adopt a low spin (LS) state [11]. This compound can then be envisaged as formed by magnetic planes with Co^{2+} ions in high spin (HS) states at sites 1, 2, and 3, separated by non-magnetic Co^{3+} ions occupying sites 4. These magnetic planes are 4.652 Å apart and the magnetic interaction between them takes place only through the bonding $Co^{2+} - O - O - Co^{2+}$ or $Co^{2+} - O - Co^{3+}(LS) - O - Co^{2+}$. This is expected to be less effective than the hypothetical case where sites 4 are occupied by magnetic ions and explains why the magnetic transition temperature of Co_3BO_5 is much lower than that of Fe_3BO_5.

A deeper understanding of the magnetic properties of homometallic Co_3BO_5 ludwigite, can be achieved doping this system with nonmagnetic [5,6,12] and magnetic ions [7,13,14]. In the case of positional disorder, when the dopant metal ion occupies randomly all available sites, the magnetic interactions are weakened either by the presence of non-magnetic ions or by frustration arising from magnetic disorder leading to the establishment of a spin-glass state [6,7,13]. When the dopant is a nonmagnetic ion that occupies exclusively sites 4, the magnetic interactions are strengthened resulting in an increase of the magnetic transition temperature. This is the case of $Co_5Sn(BO_5)_2$ where Sn ions occupy exclusively sites 4 and the temperature of the magnetic transition drastically rises, from 42 K in pure Co_3BO_5 to 82 K in the Sn-doped compound [12]. This is one of the highest magnetic transition temperature in ludwigites with a single ordering temperature. In this compound, Sn^{4+} occupy half of the sites 4 [12] causing the remaining Co ions in sites 4 to assume the valence state 2+. That is, the LS Co^{3+} ions at sites 4 are replaced by HS Co^{2+} and non-magnetic Sn^{4+} ions. Thus, in $Co_5Sn(BO_5)_2$ ludwigite, the magnetic layers, composed of HS Co^{2+} ions at sites 1, 2 and 3, are exchange-coupled by HS Co^{2+} ions at sites 4. This, together with the absence of double exchange interactions would explain its high magnetic tran-sition temperature when compared to the homometallic, *pure* Co ludwigite. Similar results were found in Al-doped Co_3BO_5 where Al^{3+} ions occupy mostly sites 4 and the magnetic transition temperature is raised up to 57 K [5]. In this case, the presence of Co^{2+} in sites 4 that strengthens the magnetic interactions via the coupling of the magnetic layers. This arises since a small proportion of the Al^{3+} ions also prefers to occupy site 2 [5]. Roughly speaking, the difference between the magnetic transition temperature of the $Co_5Sn(BO_5)_2$ and that of the $Co_{4.76}Al_{1.24}(BO_5)_2$ seems to be related to the num-ber of HS Co^{2+} at sites 4. Attempts to place others magnetic ions solely on sites 4, in a way that strengthens magnetic interactions, have so far been unsuccessful. This occurs since, in general, magnetic ions tend to occupy more than one crystallographic site [13,15]. For example, in Co_2FeBO_5, the Fe^{3+} ions occupy distinct crystallographic sites, preferentially sites 4 followed by sites 2 [13,15]. A magnetic transition is observed at ~115 K and attributed to the partial ordering of Fe-rich regions of the $4 - 2 - 4$ ladder. This is reminiscent of the partial magnetic transition observed at 112 K in pure Fe_3BO_5 ludwigite. A peak at ~70 K in the ac susceptibility was interpreted as a spin freezing of the remaining ions [13].

Alternatively, this was associated with the wall movement of antiferrimagnetic domains [15]. No clear magnetic ordering of the spins was observed in this compound.

In this work, we will show that Cr-doping of the Co_3BO_5 ludwigite strengthens the magnetic interactions and raises the magnetic transition temperature from 42 to 76 K. The Cr^{3+} places mainly at sites 4 and seems to produce less magnetic frustration when compared to Fe-doped Co_3BO_5.

II. EXPERIMENTAL

A. Samples preparation

Polycrystals of $Co_{2.5}Cr_{0.5}BO_5$ were synthesized by con-ventional high temperature solid state reaction. Stoichiometric mixture of high-purity CoO, Cr_2O_3 and H_3BO_3 were ground using an agate mortar and pressed into pellets of 10 mm in diameter and 3-mm thickness. The heat treatment of the pellet was performed in two steps. First, to decompose the H_3BO_3, the pellet was preheated in platinum crucible for 12 h at 750 °C. Subsequently, the material was regrounded, pressed into pellets and sintered at 1050 °C for 30 h in air. In both steps, the sample was cooled down according to thermal inertia of the furnace.

B. X-ray diffraction

Room temperature x-ray powder diffraction experiments were performed in the $Co_{2.5}Cr_{0.5}BO_5$ ludwigite using the Bruker AXS D8 Advance diffractometer with the Lynx-Eye detector and Co-Kα source radiation to avoid fluores-cence. The x-ray diffraction (XRD) pattern was collected in a Bragg-Brentano configuration in the 10°-90°, 2θ range, with incremental steps of 0.02°. The XRD data were re-fined using the Rietveld method implemented in the FULL-PROF program [16]. The profile function used to adjust the shape of the diffraction peaks was the pseudo-Voigt func-tion. The refinement shows the formation of single phase $Co_{2.5}Cr_{0.5}BO_5$ with orthorhombic structure and spatial group *Pbam* (Fig 1). The refinement resulted in the stoichiometric formula $Co_{2.51}Cr_{0.49}BO_5$ and, subsequently, we named it as $Co_{2.5}Cr_{0.5}BO_5$. Figure 2(a) shows the crystal structure of $Co_{2.5}Cr_{0.5}BO_5$ projected in the *a-b* plane. All metallic ions at the four nonequivalent sites are octahedrally coordinated by oxygen atoms. Sites 1, 2, and 3 are occupied by Co^{2+} ions, while sites 4 are randomly occupied by Co^{3+} and Cr^{3+} (see below). A perspective view of the planes formed by Co^{2+} at sites 1, 2, and 3 is shown in Fig. 2(b). In the homometal-lic Co_3BO_5 ludwigite, these magnetic planes are separated by nonmagnetic Co^{3+} at sites 4, as shown in Fig. 2(a). In $Co_{2.5}Cr_{0.5}BO_5$ ludwigite these planes are coupled magneti-cally through the magnetic ions Co^{3+} and Cr^{3+} at sites 4 (see discussion below). Table I presents the crystallographic data of $Co_{2.5}Cr_{0.5}BO_5$ obtained from the refinement. For comparison, the crystal data corresponding to the Co_3BO_5 ludwigite [10] was also included in Table I. The presence of Cr in the structure was confirmed by energy dispersive x-ray spectroscopy measurements (not shown) and by the change of the lattice parameters of the $Co_{2.5}Cr_{0.5}BO_5$ in relation to that of *pure* Co_3BO_5 ludwigite (see Table I).
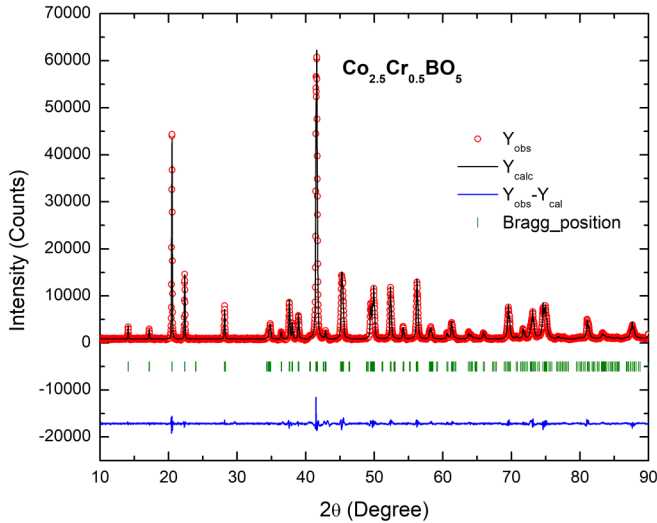
FIG. 1. Rietveld refinement of the x-ray diffraction pattern of $Co_{2.5}Cr_{0.5}BO_5$. The experimental data are represented by open red circles and the calculated pattern by the black solid lines. The difference pattern (Y_{obs}-Y_{calc}) is given by the solid blue line in the bottom of the figure. The vertical green bars show the positions of the Bragg reflections. The parameters (not corrected for background) obtained through the x-ray diffraction pattern refinement are: $R_p = 1.63$, $R_{wp} = 2.20$, $R_{exp} = 1.14$, S = 1.92, and Chi^2 = 3.75.

The refinement indicates that Cr ions are located exclusively on sites 4, occupying 49% of these sites (see Table II). Table IV displays the bond lengths between the metal ions (Co, Cr) and oxygen in an octahedral coordination (see Table III). From these distances, we can estimate the oxidation numbers for the ions in each crystallographic site by using the bond valence sum (BVS) calculations [18].
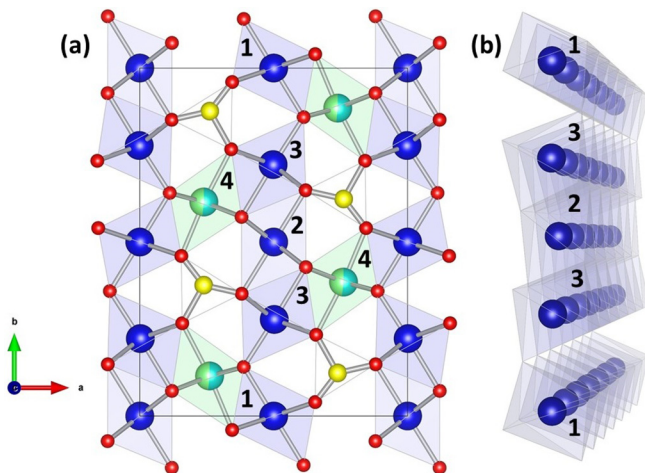

FIG. 2. (a) Crystalline structure of $Co_{2.5}Cr_{0.5}BO_5$ ludwigite projected in the a-b plane. The continuous line represents the unit cell, the yellow balls represent the boron atoms and the red ones denote the oxygen atoms. The blue, light blue, and green balls represent the Co^{2+}, Co^{3+}, and Cr^{3+} atoms, respectively. (b) Perspective view of the planes formed by Co^{2+} ions at sites 1, 2, and 3 (for a better visualization the oxygen atoms were omitted). Figures were generated by the VESTA software [17].

TABLE I. Crystallographic parameters of $Co_{2.5}Cr_{0.5}BO_5$ and Co_3BO_5 [10].

Empirical formula	$Co_{2.5}Cr_{0.5}BO_5$	Co_3BO_5
Formula weight	528.26 g/mol	535.20 g/mol
Temperature	293(2) K	293(2) K
Crystal system	Orthorhombic	Orthorhombic
Space group	*Pbam*	*Pbam*
Unit cell dimension a =	9.2934(4) Å	9.3014(3) Å
b =	12.0845(4) Å	11.9317(4) Å
c =	3.0097(5) Å	2.9627(1) Å
Volume	337.774 Å^3	329.168 Å^3
Z	4	4

Applying the formula given by Liu and Thorp [18] for the oxidation numbers Z_j of the metal ions at site j:

$$Z_j = \sum_j \exp[([r_0 - r_{ij}]/b)] \quad (1)$$

where r_0 and b are parameters given in Ref. [19] and r_{ij} are the distances between the metal ion and the oxygens in the octahedron (Table III), we got the valence state for the Co and Cr at the different sites in the structure (Table IV).

These results allow us to assign a valence state 2+ for all Co ions at sites 1, 2 and 3, the same valence state that they have in *pure* Co_3BO_5 ludwigite. In the same way, a valence state 3+ is assigned to Co and Cr at sites 4. Another parameter that gives us information about the position of Cr in the structure is the root of harmonic mean square (rhms) radius r_0 of the metallic ions [20]:

$$r_0 = \left[1/6 \sum_{i=1}^{6} 1/((d_i - 1.40)^2) \right]^{-1/2} \quad (2)$$

where 1.40 is an estimate of the oxygen radius in (Å) and d_i are the distances between the ion and the oxygens in the octahedron. The radii of the metallic ions located in the four sites of the structure are shown in Table V and, for comparison, the ionic radii of the Co ions of the Co_2CrBO_5 [Mariano *et al.* [21]] ludwigite were included. As we can see, the ionic radii of the Co at sites 1, 2, and 3 remain almost

TABLE II. Atomic coordinates (Å), site occupation factor (SOF) and U_{iso} for $Co_{2.5}Cr_{0.5}BO_5$. U_{iso} is the isotropic atomic displacement parameter (in Å^2).

Site	x/a	y/b	z/c	SOF	U_{iso}
Co(1)	1/2	0	0	1/4	0.0354(13)
Co(2)	0	0	1/2	1/4	0.0482(12)
Co(3)	0.5021(5)	0.27747(10)	0	1/2	0.0353(9)
Co(4)	0.2607(3)	0.1151(2)	1/2	0.25759	0.0406(9)
Cr(4)	0.2607(3)	0.1151(2)	1/2	0.24241	0.0406(9)
O(1)	0.3805(6)	0.3514(7)	1/2	1/2	0.009(2)
O(2)	0.3449(9)	-0.0401(8)	1/2	1/2	0.035(3)
O(3)	0.1200(8)	0.0722(6)	0	1/2	0.034(4)
O(4)	0.1586(11)	0.2667(8)	1/2	1/2	0.030(3)
O(5)	0.3883(7)	0.1410(7)	0	1/2	0.017(3)
B	0.239(2)	0.3762(16)	1/2	1/2	0.015(5)

TABLE III. Selected bond lengths between cobalt and oxygen ions in $Co_{2.5}Cr_{0.5}BO_5$. The subscripts are the symmetry codes: (i) $x - 1/2, -y + 1/2, z - 1$; (ii) $-x + 3/2, y - 1/2, -z - 1$.

Co_1-O_1	2.139(5) Å	Co_3-O_3	1.959(7) Å
Co_1-O_4	1.995(7) Å	Co_3-O_4	2.121(6) Å
Co_2-O_1	2.066(4) Å	Cr/Co_4-O_{ii}	1.941(4) Å
Co_2-O_4	2.111(7) Å	Cr/Co_4-O_2	2.060(4) Å
Co_3-O_1	2.160(7) Å	Cr/Co_4-O_3	2.062(9) Å
Co_3-O_2	2.083(5) Å	Cr/Co_4-O_{4iv}	2.032(8) Å

TABLE V. Ionic radii r_0 (rhms) of the metals at different sites in Co_3BO_5, $Co_{2.5}Cr_{0.5}BO_5$ and Co_2CrBO_5 ludwigites.

Site	Co_3BO_5 [10] $r_0(\text{Å})$	$Co_{2.5}Cr_{0.5}BO_5$ $r_0(\text{Å})$	Co_2CrBO_5 $r_0(\text{Å})$
1	0.680	0.690	0.672
2	0.671	0.695	0.688
3	0.679	0.682	0.691
4	0.563	0.608	0.650

unaffected by the Cr doping. However, the radius of the ion at site 4 has a considerable increase. Since the ionic radius of the high spin (HS) Cr^{3+} (0.615 Å) is larger than the ionic radius of the low spin (LS) Co^{3+} (0.540 Å), the increase in the ionic radius of the metal at site 4 clearly indicates that Cr^{3+} ions occupy mainly sites 4. Also, the ionic radius calculated for Co at site 4 is compatible with that of Co^{3+} in a HS state [19]. As we will show in the next section, the attribution of a high spin state for Co^{3+} at site 4 is also consistent with magnetization measurements.

C. Magnetic Measurements

The magnetization measurements were performed on powder $Co_{2.5}Cr_{0.5}BO_5$ ludwigite using a commercial Quantum Design physical properties measurement system (PPMS).

Figure 3 shows the temperature dependence of magnetization curves for field-cooled (FC) and zero-field-cooled (ZFC) protocols with a probe field of 100 Oe. In both curves, ZFC and FC, a sudden increase of magnetization takes place at ~76 K. At lower temperatures, these curves become dependent on their specific protocol. As will be shown later, the temperature of the increase in magnetization coincides with that of the rise of the specific heat and ac susceptibility. This leads us to identify this temperature as the onset of a magnetic transition. Above the magnetic transition, the magnetization decreases with increasing temperature according to a Curie-Weiss law. The linear fit of the 1 T dc susceptibility (H/M) curve (see inset) leads to a Curie constant $C = (26.46 \pm 0.02) \times 10^{-3}$ emu$Kg^{-1}Oe^{-1}$ and Curie-Weiss temperature $\theta_{CW} = -(65.6 \pm 0.3)$ K. The predominance of antiferromagnetic interactions is evidenced by the negative value of the Curie-Weiss temperature. Using the value of the Curie constant, we obtain the effective magnetic moment per unit formula $p_{eff} = 7.50$ μ_B for the $Co_{2.5}Cr_{0.5}BO_5$ ludwigite. The calculation of the mean effective magnetic moment

TABLE IV. Oxidation number Z for the four crystallographic sites of $Co_{2.5}Cr_{0.5}BO_5$ ludwigite obtained through BVS calculations [18].

Site	Ion	Z
1	Co1	2.074
2	Co2	2.097
3	Co3	2.060
4	Co4(Cr4)	2.581(2.754)

per unit formula, considering only the spin momentum ($g = 2$) for Co^{2+} ($S = 3/2$) and Cr^{3+} ($S = 3/2$), gives $\mu_s = \sqrt{(\sum_i n_i g_i^2 S_i(S_i + 1))} = 6.11\mu_B$ (with $n_{Co^{2+}} = 2$ and $n_{Cr^{3+}} = 0.49$ ions per formula unit). On the other hand, if we consider the Co^{3+} at sites 4 ($n_{Co^{3+}} = 0.51$) in a HS state ($S = 2$), we get $\mu_S = 7.04$ μ_B. A value somewhat smaller than that found experimentally. The difference may arise since we neglected the contribution of the orbital moment of Co^{2+} which, in the Co ludwigite is not completely quenched [10].

Figure 4 displays the magnetic hysteresis loops for $Co_{2.5}Cr_{0.5}BO_5$ at different temperatures. Below 80 K the magnetization has no longer a linear dependence with the applied field and the hysteresis curves begin to open, consistent with a ferro- or ferrimagnetic ordering. The remanent magnetization and coercive field increase as the temperature decreases (Fig. 4). In the 10 K hysteresis loop a rounded step is observed at ~4 T, indicating a possible metamagnetic transition. At 2 K, the step is more evident and a jump in magnetization occurs at 5 T. The 2 K hysteresis curve has a remanent magnetization of 2.0 μ_B/f.u. and a coercive field of about ~2.2 T. The large value of the coercive field indicates strong anisotropic effects, commonly found in ludwigites [12]. The magnetization at 2 K and 9 T is 3.4 μ_B/f.u., a similar value found for the Sn-doped ludwigite under the same conditions.

Figure 5 presents the temperature dependence of the real (χ') and imaginary part (χ'') of the ac susceptibility measurements of $Co_{2.5}Cr_{0.5}BO_5$ for different frequencies. As the
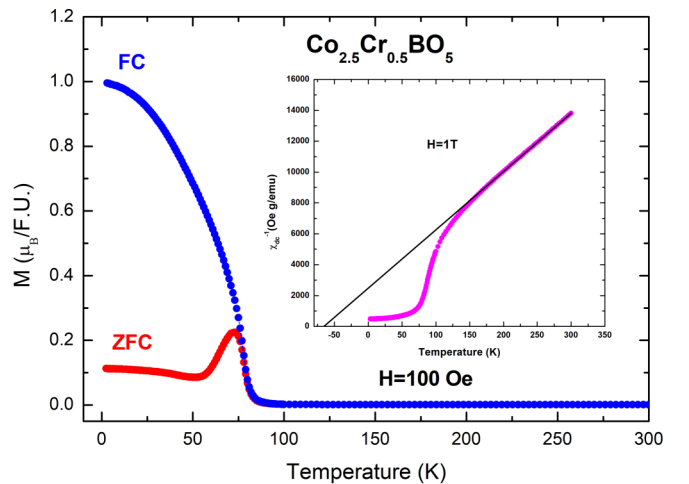

FIG. 3. Magnetization versus temperature of $Co_{2.5}Cr_{0.5}BO_5$ ludwigite under a probe field of 100 Oe. Inset: Inverse magnetization in a 1 T magnetic field.

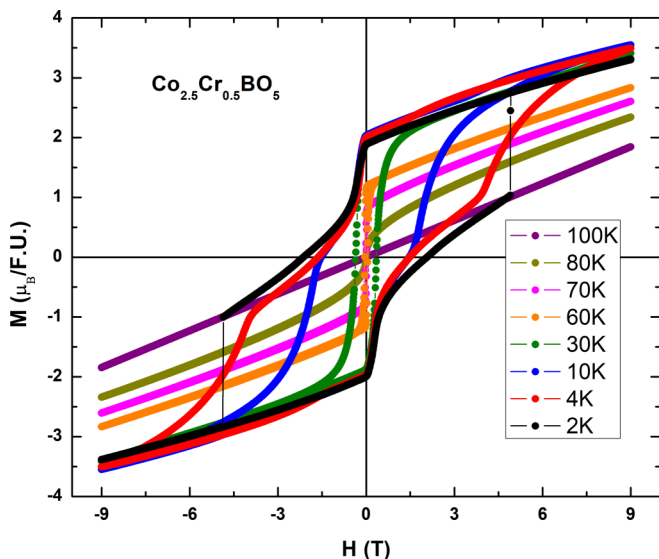FIG. 4. Hysteresis loops for powdered $Co_{2.5}Cr_{0.5}BO_5$ compound at 2, 4, 10, 30, 60, 70, 80, 100 K.

FIG. 6. Specific heat of $Co_{2.5}Cr_{0.5}BO_5$ represented as C/T versus T for 0, 4, and 9 T fields. Inset: Zoom of the region where the intersection of the curves for different fields occurs.

temperature is lowered, near 83 K, a substantial increase of the ac susceptibility is observed, reaching a maximum at 76 K. The position of the peak, centered at 76 K, slightly shifts to higher temperatures as the frequency increases (about 0.01 K for two decades change in frequency). If we assume
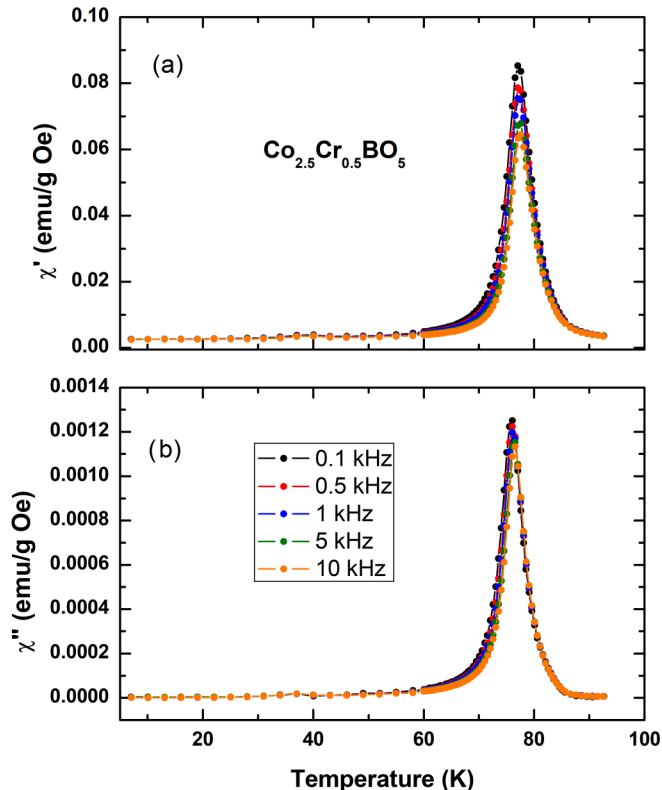

FIG. 5. Real part of the ac magnetic susceptibility of $Co_{2.5}Cr_{0.5}BO_5$ (a) and its imaginary part (b) as functions of temperature for 0.1, 0.5, 1, 5, and 10 kHz. The amplitude of the oscillating magnetic field is 10 Oe.
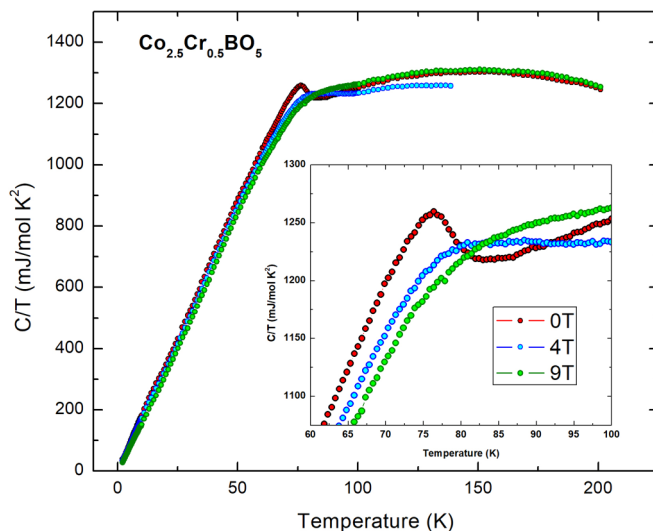
that this peak corresponds to a spin glass transition, its shift position with frequency could be analyzed with the critical dynamic scaling law [22]. The best fit to the power law yields $T_g = 77$ K, $\tau_0 = 3.5 \times 10^{-14}$ s and a critical exponent $z\nu = 4.0$. Considering that typical values of $z\nu$ for spin glass systems lie between 5 and 11 [23], these results indicate the lack of spin-glass-like phase transition in $Co_{2.5}Cr_{0.5}BO_5$. This small variation of the position of the peak with the frequency probably has its origin in the dynamics of the spins in domain walls [24].

D. Heat Capacity

Specific-heat measurements as a function of temperature ($2 \leqslant T \leqslant 200$ K) were performed using a commercial Quantum Design Dynacool PPMS. 5 mg pellets of $Co_{2.5}Cr_{0.5}BO_5$ powder were used. Figure 6 displays specific heat curves plotted as C/T versus T for applied magnetic fields of 0, 4, and 9 T. Lowering the temperature an inflection point in the specific heat curve is observed at ~ 76 K. This is the same temperature where considerable increases in the magnetization and ac susceptibility values occur. So, we defined this temperature as the onset of the magnetic ordering. The peak at 76 K smooths down and shifts to higher temperatures with the applied magnetic field, indicating the ferro or ferrimagnetic nature of the magnetic transition.

This magnetic ordering temperature is comparable only with that of the Sn-doped ludwigite, considered, until now, the highest transition ordering temperature among the ludwigites [12].

For low temperatures (T < 6 K) the temperature dependence of the heat capacity is well described by the expression $C = \delta T^{3/2} + \beta T^3$ (Fig 7). The fitting parameters are shown in Table VI. The analysis of results in an applied magnetic field requires that we include the modification due to a Zeemann gap Δ in the previous expression. This is now given by, $C = \delta T^{3/2} e^{-\Delta/T} + \beta T^3$. The $T^{3/2}$ term is due to ferromagnetic

TABLE VI. The γ, δ, Δ, α, β, and θ_D parameters obtained from the fits of the low temperature specific heat data (Fig. 7) of Cr-doped $Co_{2.5}Cr_{0.5}BO_5$ ludwigite. For comparison, the parameters of other ludwigites are also presented. The general equation used for the fits is $C = \gamma T + \delta T^{3/2} e^{-(\Delta/T)} + \alpha T^2 + \beta T^3$.

Compound	$H(T)$	γ(mJ/mol K^2)	δ(mJ/mol K$^{5/2}$)	Δ(K)	α(mJ/mol K^3)	β(mJ/mol K^4)	θ_D (K)
$Co_{2.5}Cr_{0.5}BO_5$	0	-	21.23 ± 0.11	-	-	1.60 ± 0.01	106.36
	4	-	20.49 ± 0.20	-	-	1.52 ± 0.02	108.41
	9	-	25.92 ± 2.04	1.00 ± 0.14	-	1.12 ± 0.10	135.36
Co_3BO_5	0	-	-	-	4.05 ± 0.11	0.85 ± 0.02	114.95
$Co_5Sn(BO_5)_2$[12]	0	0.54 ± 0.02	-	-	-	0.650 ± 0.002	144
	9	0.00 ± 0.02	-	-	-	0.656 ± 0.002	143
$Co_5Ti(BO_5)_2$ [6]	0	15.03	-	-	-	3.94	79
	4	6.88	-	-	-	2.78	89
	9	3.61	-	-	-	2.76	89
$Co_{4.76}Al_{1.24}(BO_5)_2$ [5]	0	-	-	-	1.94	-	-
	9	-	-	-	2.95	-	-

magnons in a three dimensional system [25] and the T^3 term is due to lattice phonons [25]. The latter contribution is expected to be small for this range of temperature. We point out that this ferromagnetic magnon contribution to the specific heat had not been observed previously in any ludwigite.

III. DISCUSSION

X-ray powder diffraction results have shown that in the Cr-doped $Co_{2.5}Cr_{0.5}BO_5$ compound, the Cr ions occupy mainly sites 4 of the ludwigite structure. These sites 4 are randomly occupied by Cr and Co ions in the ratio 1:1. BVS calculations allowed us to ascribe a 2+ valence number to all the Co ions at sites 1, 2 and 3. Furthermore, their calculated ionic radii are consistent with a high spin state (HS) for these three sites as in the parent *pure* Co_3BO_5 ludwigite. For sites 4, a valence state of 3+ is attributed to both Cr and Co ions. Differently from Co_3BO_5, where the Co^{3+} ions at site 4 are

FIG. 7. Low temperature fit of the specific heat represented as C versus T for 0, 4, and 9 T for $Co_{2.5}Cr_{0.5}BO_5$. The parameters obtained from the fits of the curves are shown in Table VI.

in a LS state, in $Co_{2.5}Cr_{0.5}BO_5$ the calculated ionic radius indicates that the Co^{3+} at sites 4 are in a HS state. Recent x-ray diffraction, x-ray absorption spectroscopy, and magnetization experiments in Co_3BO_5 suggest a gradual Co^{3+} spin-state crossover (from LS to HS state as the temperature rises) below 300 K [26]. In addition, magnetization measurements above 300 K are consistent with a HS state for Co^{3+}. This spin state is stabilized by thermal expansion of the $Co^{3+} - O$ bonds that reduces the crystal electric field splitting between the t_{2g} and e_g levels [26]. The volume of the unit cell of Cr-doped $Co_{2.5}Cr_{0.5}BO_5$ (338.0 Å^3) corresponds to that of Co_3BO_5 at a temperature of $\sim$500 K [26]. Since Cr substitution has a similar effect to that caused by thermal expansion in the Co_3BO_5, it is realistic to attribute a HS state to Co^{3+} in the Cr-doped $Co_{2.5}Cr_{0.5}BO_5$. In fact, the average $Co - O$ distances (2.023 Å) for Co occupying sites 4 in $Co_{2.5}Cr_{0.5}BO_5$ is larger than that of Co_3BO_5 (1.962 Å) at room temperature. Consequently, a HS state for the Co^{3+} is preferred in the former [27,28]. As will be discussed further on, these results are also consistent with magnetization experiments in the pure compound. Thus, the increase of the lattice parameters in Cr-doped $Co_{2.5}Cr_{0.5}BO_5$ can be attributed to the larger ionic radius of Cr^{3+} (0.615 Å). This is associated with the larger ionic radius of the high spin state of Co^{3+} (0.610 Å) compared with that of the low spin Co^{3+} (0.545 Å) at site 4 in the pure ludwigite.

The effective moment per formula unit, obtained from the Curie-Weiss fit of the magnetic susceptibility in the paramagnetic region (T > 200 K) (inset of Fig 3), is $p_{eff} = 7.50 \mu_B$. The estimated spin-only moment considering all the ions in a high spin state is $\mu_S = 7.04 \mu_B$, a value close to the experimental one. The small difference may be due to the orbital magnetic moment contribution of the Co^{2+} ions. This has been observed in selected compounds where the Co^{2+} is octahedrally coordinated by oxygen ions [29,30]. Consequently, the magnetic results are consistent with those of x-ray diffraction that indicate a HS state for the Co^{3+} at sites 4.

The low energy magnetic excitations of the ferrimagnetic state are long wavelength spin waves with a quadratic dispersion $\varepsilon_k = \Delta + Dk^2$. The stiffness coefficient D is related to the coefficient of the $T^{3/2}$ law of the decrease of
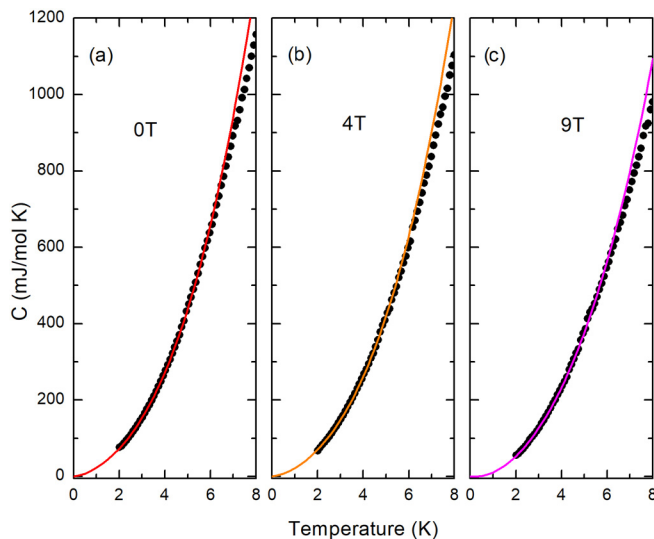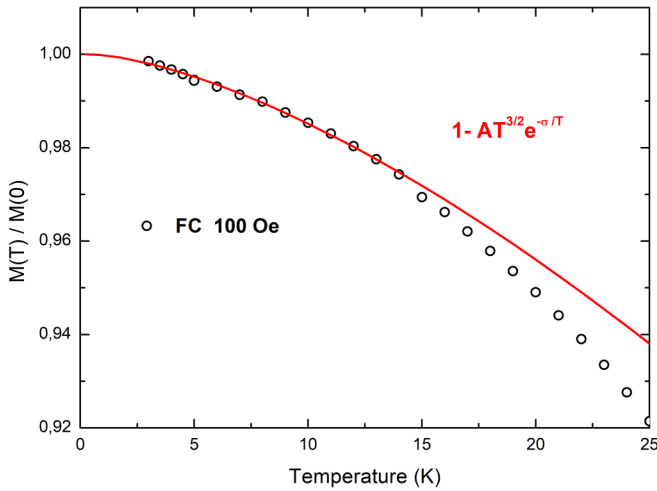
FIG. 8. Fit of the temperature dependent FC magnetization of $Co_{2.5}Cr_{0.5}BO_5$ at 100 Oe. This is shown as $M(T)/M(0)$ versus T. The constants obtained from the fit are $A = 5.143 \times 10^{-4} K^{-3/2}$ and $\sigma = 0.909$ K.

the magnetization with temperature in the low-temperature region [31]:

$$\frac{M(T)}{M_0} = 1 - \frac{0.0587}{\bar{N}_0|S_a - S_b|}\left(\frac{k_B T}{D}\right)^{3/2}, \qquad (3)$$

where $\bar{N}_0 = N_0/V$ is the number of magnetic atoms per unit volume and S_a and S_b are the spins of the two sub-lattice systems. The temperature dependence of the magnetization under an applied field of 100 Oe is shown in Fig 8. The low temperature results are well fitted with the expression $M(T)/M_0 = 1 - AT^{3/2}e^{-\sigma/T}$. The spin-wave stiffness D may be calculated from the parameter A via the relation $A = \frac{0.0587}{\bar{N}_0|S_a - S_b|}(\frac{k_B}{D})^{3/2}$. Using $\bar{N}_0|S_a - S_b| = |4S(Co^{2+}) - S(Co^{3+}) + S(Cr^{3+})|/V = 16.28 \times 10^{-3} Å^{-3}$ for Cr-doped $Co_{2.5}Cr_{0.5}BO_5$ (assuming a ferrimagnetic structure, as described below) and $A = 5.143 \times 10^{-4} K^{-3/2}$ from the fit, we obtain $D = 32$ meV$Å^2$. This value is similar to that found by specific heat measurements, showing the consistence of the present analysis.

The magnetization curves shown in Fig. 4 present, below 30 K, the form of constricted hysteresis cycles, characterized by small remanence, low permeability at coercive fields and weak field dependence of the magnetic susceptibility at low fields. This behavior is observed in some ferro- and ferrimagnetic systems and may have different causes. In metallic ferromagnets, it has even been attributed to eddy currents [32]. In insulating materials, such as ours, it has been related to short range order and/or the existence of neighboring uniaxial domains whose axes are perpendicular and their boundary bisects the angle between them [33]. The net effect is to reduce the domain wall mobility. Further work, outside the scope of this paper is necessary to unravel the nature of this phenomenon in the present ludwigite.

The Cr-doped $Co_{2.5}Cr_{0.5}BO_5$ system has long-range magnetic order below $T_C \sim 76$ K. This is shown by the presence of a peak in the specific-heat (see inset of Fig 6) and also a narrow peak in the ac susceptibility at this temperature. The latter does not shift with a change of two decades in

frequency (see Fig 5). The absence of a linear temperature dependent term in the specific heat C_p at low temperatures and the smallness of the *frustration parameter* $|\theta_{CW}|/T_C$ (with $\theta_{CW} = -87.91$ K and T_C taken as 76 K) close to unity indicate that $Co_{2.5}Cr_{0.5}BO_5$ presents true long range magnetic order and not a freezing of the moments. The nature of the magnetic spin arrangement in the magnetically ordered state is given by the result of the analysis of the specific heat data at low temperatures (<5 K). The $T^{3/2}$ term in the temperature dependence of the specific heat reflects a three-dimensional ferro- or ferrimagnetic ordering [25]. Correspondingly, we can see in Fig. 6 that magnetic field reduces significantly the total heat capacity of the Cr-doped $Co_{2.5}Cr_{0.5}BO_5$ and that this reduction does not level off even at highest field available (9 T). This behavior is typical of a ferromagnet in which the entropy is shifted from below the Curie temperature to well above it. This shift above the Curie temperature is clearly observed in Fig 6. Near the ordering temperature, the magnetic fields drastically affects the heat capacity. The peak at 76 K for zero field shifts towards higher temperatures, becomes remarkably broader, and decreases in magnitude when the external magnetic field is 4 T. A further increase of the field continues to affect this maximum. For 9 T, the peak is hardly seen and there is no evidence of the ferrimagnetic ordering peak.

In ferrimagnets with anisotropy or in an external applied magnetic field, the low energy spin waves have a dispersion relation $\varepsilon_k = \Delta + Dk^2$, where D is the spin-wave stiffness coefficient and Δ is a gap for excitations. The specific heat per unit volume is given by $C_v = 0.113k_B(k_B T/D)^{3/2}$ [31]. The coefficient δ of our fit may be expressed as $\delta = 0.113RV(k_B/D)^{3/2}$ where R is the ideal gas constant and V is the unit cell volume. Our result yields $D = 52$ meV$Å^2$ for the Cr-doped $Co_{2.5}Cr_{0.5}BO_5$, a stiffness coefficient value comparable with that found in ferromagnetic manganites [34].

The remanent magnetization and the high coercive field at low temperatures (~ 2 T at 2 K) are also consistent with a ferro- or ferrimagnetic spin structure. The magnetic transition temperature of Cr-doped $Co_{2.5}Cr_{0.5}BO_5$ is comparable with that of the Sn-doped $Co_5Sn(BO_5)_2$ [12]. Then, doping Co_3BO_5 with non-magnetic Sn and magnetic Cr ions has almost the same effect of increasing substantially the magnetic transition temperature. The reason for this seems to be intimately related to the presence of magnetic ions at site 4. Co_3BO_5 can be seen as formed by magnetic planes formed by HS Co^{2+} at sites 1, 2, and 3 [11] separated by nonmagnetic LS Co^{3+} ions. These magnetic planes are 4.884 Å apart and weakly interacting via the $Co^{2+} - O - O - Co^{2+}$ or $Co^{2+} - O - Co^{3+}(LS) - O - Co^{2+}$ bonds. The two-dimensional nature of the magnetic state of this compound was checked through a more careful analysis of the low temperature specific heat data (Fig. 9).

In the pure system Co_3BO_5, the dominant low temperature T^2 dependence of the specific heat, which due to two-dimensional AF magnons, has shown the two dimensional character of the magnetism in this system, in agreement with neutrons studies [11]. The doping of pure Co_3BO_5 with nonmagnetic Sn considerably increases the magnetic transition temperature, almost doubling its value that reaches
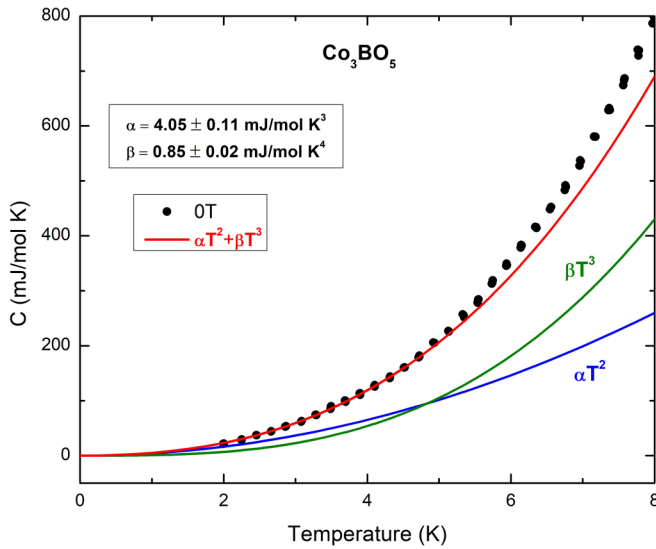
FIG. 9. Specific heat of the pure Co_3BO_5 represented as *C* versus *T* for 0 T. The parameters of the fits are shown in Table VI. The data used for the heat capacity fit were obtained from the literature [10].

82 K [12]. This is the highest magnetic transition temperature for the ordering of all moments in a ludwigite [12]. This dramatic effect can be explained since in Sn-doped $Co_5Sn(BO_5)_2$, Sn ions occupy exclusively sites 4. This forces the remaining Co ions in this site to adopt a valence 2+ and a HS state. The appearance of Co^{2+} in sites 4, previously occupied by low spin Co^{3+}, strongly couples the magnetic layers, without increasing frustration of the magnetic interactions [12]. As a consequence, this type of doping strengthens the magnetic interactions raising the magnetic transition temperature.

In Cr-doped $Co_{2.5}Cr_{0.5}BO_5$ compound, the situation is similar. Sites 1, 2 and 3 preserve the high spin Co^{2+} and sites 4 are now occupied by two magnetic ions in a HS state, Cr^{3+} ($S = 3/2$) and Co^{3+} ($S = 2$), coupling the magnetic planes. The presence of these ions with different electronic and spin configurations actually increases the number of possible magnetic interactions, when compared with those in the Sn-doped $Co_5Sn(BO_5)_2$ and gives rise to additional magnetic frustration. However, this does not seem to be relevant and the magnetic interactions are strengthened leading to a magnetic order throughout the compound at 76 K. These arguments are supported by the analysis of the low temperature specific heat data, which indicated a two-dimensional antiferromagnetic (AFM) state in Co_3BO_5 (T^2 dependence of the specific heat) that upon Cr-doping displays a three-dimensional ferro- or ferrimagnetic behavior ($T^{3/2}$ dependence of the specific heat).

Despite that our system presents three magnetic ions Co^{2+}, Co^{3+}, and Cr^{3+} with different electronic and spin configurations, a more detailed magnetic structure can be suggested. We start by analyzing ladder $4 - 2 - 4$, where three different magnetic ions are located. In this ladder, the shortest distances between the ions take place and the strongest interactions are expected. Sites 2 are occupied exclusively by HS Co^{2+}, which are magnetically coupled via $90°$ $Co^{2+} - O - Co^{2+}$ superexchange interactions (J_1 in Fig 10). Sites 4 are randomly occupied by Co^{3+} and Cr^{3+}, consequently increasing
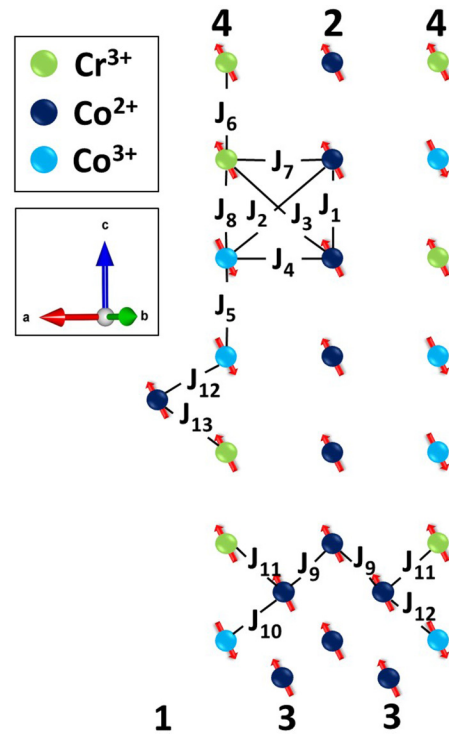

FIG. 10. Scheme for superexchange interactions and magnetic order in the $4 - 2 - 4$ ladder of Cr-doped $Co_{2.5}Cr_{0.5}BO_5$ ludwigite. Sites 1 and 3 are at different depths of the $4 - 2 - 4$ ladder.

the number of possible exchange interactions. So, in this configuration, we have now 180^0 $Co^{3+} - O - Co^{2+}(J_2)$ and $Cr^{3+} - O - Co^{2+}(J_3)$; 90^0 $Co^{3+} - O - Co^{2+}(J_4)$, $Co^{3+} - O - Co^{3+}(J_5)$, $Cr^{3+} - O - Cr^{3+}(J_6)$, $Cr^{3+} - O - Co^{2+}(J_7)$, and $Cr^{3+} - O - Co^{3+}(J_8)$ superexchange interactions. Calculations of superexchange integrals [35] as well as experimental results of Mössbauer spectroscopy in CoSn ludwigite [12] and NiSn hulsite [36] have shown that $180°$ M $- O - M$ exchange interactions are generally dominant in this type of compound. These calculations also show that the J_2 is AFM. Goodenough-Kanamori (G-K) rules predict a FM exchange interaction for J_3 [37]. Assuming that these two interactions determine the magnetic order in the Cr-doped system, the coupling between the Co^{2+} ions along the *c* axis should be FM (J_1), exactly as predicted by the exchange integral calculations [35]. The same calculations indicate an AFM interaction for J_4 and J_5. While J_4 satisfies the proposed spin configuration shown in Fig. 10, the latter generates magnetic frustration. On the other hand, a spin configuration with a FM coupling for J_5 has the lowest energy [35]. In addition, such a FM configuration agrees with the G-K rules. The sign of J_5 can be reversed if strong simultaneous interactions of $180°$ take place [37]. However, this is not the case since the strong J_2 AFM coupling holds J_5 FM. Thus, a FM coupling for J_5 is possible. Due to the random distribution of Cr^{3+} and Co^{3+} ions at sites 4, $90°$ superexchange interactions Cr-Cr (J_6) and Cr-Co $(J_7$ and $J_8)$ are possible. According to G-K rules, J_6 and J_7 should be FM [37,38] satisfying the proposed spin configuration. Moreover, according to the G-K rules the J_8 coupling should be FM, generating frustration in

our proposed model. On the other hand, an AFM coupling may be predominant for larger $Co^{3+} - Cr^{3+}$ separations [37]. This is precisely the case. Notice the ferrimagnetic state experimentally supported by the presence of two different ions (Cr^{+3} and Co^{+3} at sites 4 and the negative θ_{CW} value found in the magnetization experiments. As a whole, there are only two interactions that could produce frustration in the $4 - 2 - 4$ ladder. Calculations of superexchange interactions indicate a FM coupling between Co^{2+} at sites 2 and 3 (J_9) and AFM between the Co^{3+} at site 4 and the Co^{2+} at site 3 (J_{10}). These imply a FM coupling between Cr^{3+} at site 4 and Co^{2+} at site 3 (J_{11}) that is in full agreement with the G-K rules [37]. Finally, the AFM coupling between Co^{3+} at sites 4 and Co^{2+} at sites 1 (J_{12})as suggested by calculations [35], implies a FM coupling between Cr^{3+} at site 4 and Co^{2+} at site 1 (J_{13}), in total agreement with the G-K rules. Thus, a ferrimagnetic structure is formed that is consistent with the G-K rules and the superexchange interaction calculations. The proposed magnetic structure is also in agreement with the experimental results obtained here.

A full characterization of the magnetic interactions remains a subtle problem in spite of the success of the direct and indirect mechanisms proposed to explain the magnetic behavior in several systems. Particularly in ludwigites, exchange interaction calculations properly describe the experimentally observed magnetic behaviors of several of these systems [39–43]. Doping homometallic Co_3BO_5 ludwigite with magnetic ions can lead, not necessarily to a change in the exchange interaction sign but to a change in the interaction strength [39]. Exchange interaction calculations for $Co_{2.5}Cr_{0.5}BO_5$ will be helpful to validate the proposed magnetic structure, which in turn is consistent with the experimental results obtained in this work.

IV. CONCLUSIONS

We have demonstrated that Cr-doping Co_3BO_5 strengthens the magnetic interactions, raising the magnetic transition temperature of 42 K of this system to 76 K for the Cr-doped $Co_{2.5}Cr_{0.5}BO_5$. This drastic change occurs because Cr ions mainly occupy sites 4 of the ludwigite structure, replacing a fraction of the Co^{3+}. This causes the remaining Co^{3+} at these sites to assume a high spin state. It would be expected that in Cr-doped $Co_{2.5}Cr_{0.5}BO_5$ the presence of three magnetic ions (Co^{2+}, Co^{3+} and Cr^{3+}) with different electronic and spin configurations would increase the number of frustrating exchange interactions and decrease the magnetic transition temperature. However, the specific position of the Cr^{3+} and Co^{3+} at sites 4, in agreement with exchange interactions calculations and the G-K rules, generates few frustrated bonds and long-range magnetic order sets in at 76 K. Magnetization and specific heat results are consistent with a ferrimagnetic structure for Cr-doped $Co_{2.5}Cr_{0.5}BO_5$. The analysis of the low temperature specific heat data has shown that the two-dimensional magnetic character of pure Co_3BO_5 ludwigite changes to three dimensional when Co^{2+} is substituted by Cr^{3+}.

[1] M. Mir, R. B. Guimarães, J. C. Fernandes, M. A. Continentino, A. C. Doriguetto, Y. P. Mascarenhas, J. Ellena, E. E. Castellano, R. S. Freitas, and L. Ghivelder, Phys. Rev. Lett. **87**, 147201 (2001).

[2] J. Larrea J., D. R. Sánchez, F. J. Litterst, E. M. Baggio-Saitovich, J. C. Fernandes, R. B. Guimarães, and M. A. Continentino, Phys. Rev. B **70**, 174452 (2004).

[3] P. Bordet and E. Suard, Phys. Rev. B **79**, 144408 (2009).

[4] R. B. Guimarães, M. Mir, J. C. Fernandes, M. A. Continentino, H. A. Borges, G. Cernicchiaro, M. B. Fontes, D. R. S. Candela, and E. Baggio-Saitovich, Phys. Rev. B **60**, 6617 (1999).

[5] C. P. C. Medrano, D. C. Freitas, E. C. Passamani, C. B. Pinheiro, E. Baggio-Saitovich, M. A. Continentino, and D. R. Sanchez, Phys. Rev. B **95**, 214419 (2017).

[6] D. C. Freitas, R. B. Guimarães, D. R. Sanchez, J. C. Fernandes, M. A. Continentino, J. Ellena, A. Kitada, H. Kageyama, A. Matsuo, K. Kindo *et al.*, Phys. Rev. B **81**, 024432 (2010).

[7] Y. Knyazev, N. Ivanova, N. Kazak, M. Platunov, L. Bezmaternykh, D. Velikanov, D. Vasiliev, S. Ovchinnikov, and G. Yurkin, J. Magn. Magn. Mater. **324**, 923 (2012).

[8] E. dos Santos, D. Freitas, I. Fier, J. Fernandes, M. Continentino, A. de Oliveira, and L. Walmsley, J. Phys. Chem. Solids **90**, 65 (2016).

[9] Q. Ping, B. Xu, X. Ma, J. Tian, and B. Wang, Dalton Trans. **48**, 5741 (2019).

[10] D. C. Freitas, M. A. Continentino, R. B. Guimarães, J. C. Fernandes, J. Ellena, and L. Ghivelder, Phys. Rev. B **77**, 184422 (2008).

[11] D. C. Freitas, C. P. C. Medrano, D. R. Sanchez, M. N. Regueiro, J. A. Rodríguez-Velamazán, and M. A. Continentino, Phys. Rev. B **94**, 174409 (2016).

[12] C. P. Contreras Medrano, D. C. Freitas, D. R. Sanchez, C. B. Pinheiro, G. G. Eslava, L. Ghivelder, and M. A. Continentino, Phys. Rev. B **91**, 054402 (2015).

[13] D. C. Freitas, M. A. Continentino, R. B. Guimarães, J. C. Fernandes, E. P. Oliveira, R. E. Santelli, J. Ellena, G. G. Eslava, and L. Ghivelder, Phys. Rev. B **79**, 134437 (2009).

[14] M. A. V. Heringer, D. L. Mariano, D. C. Freitas, E. Baggio-Saitovich, M. A. Continentino, and D. R. Sanchez, Phys. Rev. Mater. **4**, 064412 (2020).

[15] J. Bartolomé, A. Arauzo, N. V. Kazak, N. B. Ivanova, S. G. Ovchinnikov, Y. V. Knyazev, and I. S. Lyubutin, Phys. Rev. B **83**, 144426 (2011).

[16] J. Rodríguez-Carvajal, *Laboratoire Léon Brillouin* (CEA-CNRS), Saclay, France (2001).

[17] K. Momma and F. Izumi, J. Appl. Crystallogr. **41**, 653 (2008).

[18] W. Liu and H. H. Thorp, Inorg. Chem. **32**, 4102 (1993).

[19] R. D. Shannon, Acta Crystallogr. Sect. A **32**, 751 (1976).

[20] R. Norrestam, M. Kritikos, and A. Sjödin, J. Solid State Chem. **114**, 311 (1995).

[21] D. L. Mariano *et al.* (unpublished).

[22] K. Binder and A. P. Young, Phys. Rev. B **29**, 2864 (1984).

[23] T. Lookman and X. Ren, *Frustrated Materials and Ferroic Glasses*, Springer Series in Materials Science (Springer, Berlin, 2018).

[24] A. Morrish, *The Physical Principles of Magnetism* (Wiley, New York, 2001).

[25] C. Enss and S. Hunklinger, *Low-Temperature Physics*, SpringerLink: Springer e-Books (Springer, Berlin, 2005).

[26] C. W. Galdino, D. C. Freitas, C. P. C. Medrano, R. Tartaglia, D. Rigitano, J. F. Oliveira, A. A. Mendonça, L. Ghivelder, M. A. Continentino, D. R. Sanchez *et al.*, Phys. Rev. B **100**, 165138 (2019).

[27] J.-M. Chen, Y.-Y. Chin, M. Valldor, Z. Hu, J.-M. Lee, S.-C. Haw, N. Hiraoka, H. Ishii, C.-W. Pao, K.-D. Tsuei *et al.*, J. Am. Chem. Soc. **136**, 1514 (2014).

[28] M. W. Haverkort, Z. Hu, J. C. Cezar, T. Burnus, H. Hartmann, M. Reuther, C. Zobel, T. Lorenz, A. Tanaka, N. B. Brookes *et al.*, Phys. Rev. Lett. **97**, 176405 (2006).

[29] J. T. Richardson and L. W. Vernon, J. Phys. Chem. **62**, 1153 (1958).

[30] A. L. Arduini, M. Garnett, R. C. Thompson, and T. C. T. Wong, Can. J. Chem. **53**, 3812 (1975).

[31] S. Flügge, *Encyclopedia of physics*, Handbuch Der Physik (Springer, Berlin, 1966).

[32] S. Takahashi, S. Kobayashi, and T. Shishido, J. Magn. Magn. Mater. **322**, 3658 (2010).

[33] S. Kaya, Rev. Mod. Phys. **25**, 49 (1953).

[34] M. B. Salamon and M. Jaime, Rev. Mod. Phys. **73**, 583 (2001).

[35] Y. Knyazev, N. Kazak, I. Nazarenko, S. Sofronova, N. Rostovtsev, J. Bartolomé, A. Arauzo, and S. Ovchinnikov, J. Magn. Magn. Mater. **474**, 493 (2019).

[36] C. P. C. Medrano, D. C. Freitas, E. C. Passamani, J. A. L. C. Resende, M. Alzamora, E. Granado, C. W. Galdino, E. Baggio-Saitovitch, M. A. Continentino, and D. R. Sanchez, Phys. Rev. B **98**, 054435 (2018).

[37] J. B. Goodenough, *Magnetism and the Chemical Bond*, Inter-science Monographs on Chemistry (R. E. Krieger, Malabar, FL, 1976).

[38] J. Kanamori, J. Phys. Chem. Solids **10**, 87 (1959).

[39] N. Kazak, N. Ivanova, O. Bayukov, S. Ovchinnikov, A. Vasiliev, V. Rudenko, J. Bartolomé, A. Arauzo, and Y. Knyazev, J. Magn. Magn. Mater. **323**, 521 (2011).

[40] G. A. Petrakovskiǐ, L. N. Bezmaternykh, D. A. Velikanov, A. M. Vorotynov, O. A. Bayukov, and M. Schneider, Phys. Solid State **51**, 2077 (2009).

[41] S. Sofronova, E. Moshkina, I. Nazarenko, A. Veligzhanin, M. Molokeev, E. Eremin, and L. Bezmaternykh, J. Magn. Magn. Mater. **465**, 201 (2018).

[42] E. Moshkina, S. Sofronova, A. Veligzhanin, M. Molokeev, I. Nazarenko, E. Eremin, and L. Bezmaternykh, J. Magn. Magn. Mater. **402**, 69 (2016).

[43] S. Sofronova, L. Bezmaternykh, E. Eremin, I. Nazarenko, N. Volkov, A. Kartashev, and E. Moshkina, J. Magn. Magn. Mater. **401**, 217 (2016).